Iranian Journal of Science and Technology, Transactions of Civil Engineering
https://doi.org/10.1007/s40996-025-01951-x

RESEARCH PAPER

Seismic Response Assessment of Topside Equipment on Fixed Offshore Platforms

Ashraf Huseynli[1] · Sezer Öztürk[2] · Bülent Erkmen[3] · Ali Sari[4]

Received: 7 May 2025 / Accepted: 25 June 2025

Abstract

The seismic performance of large equipment on offshore oil production platforms is vital for ensuring personnel safety and maintaining the structural integrity of the platform. Seismic failure of equipment can result in catastrophic hazards such as explosions, platform damage or collapse, significant economic losses, and environmental disasters. This paper evaluates the seismic performance of various types of commonly used equipment on offshore platforms in upstream operations. The seismic response of the equipment, modeled together with the platform, is assessed using nonlinear time-history analysis under three-component, 22 different high-magnitude recorded earthquake records, and analyzed through both coupled and uncoupled dynamic analyses. The findings reveal that offshore earthquakes significantly affect equipment on offshore platforms, with results indicating a positive correlation between peak ground acceleration (PGA) and material yielding in equipment supports, while peak ground velocity (PGV) and the PGA/PGV ratio significantly affect the seismic performance of the platform. Equipment that is horizontally positioned and supported is found to be more vulnerable than vertically positioned equipment, regardless of the first mode shape. The findings of this study establish seismic design recommendations for topside equipment, propose specific PGA thresholds for various types of equipment, and provide recommendations for enhanced equipment saddle designs to improve the seismic performance of topside equipment on offshore platforms.

Keywords Offshore platform · Topside equipment · Seismic design · Support design · Finite element analysis

1 Introduction

The increasing demand for hydrocarbon resources and the depletion of onshore reserves have significantly intensified the development and reliance on offshore structures, such as oil and gas platforms (Singh et al. 2020). These structures are often situated in challenging environments and are exposed to various natural hazards, including strong seismic events (Randolph and Gourvenec 2011;). As global energy demand continues to rise and exploration extends into deeper waters, ensuring the safety and resilience of offshore structures during seismic events becomes increasingly critical.

Offshore platforms typically accommodate a wide array of equipment, including storage tanks for hydrocarbons such as crude oil and natural gas condensate, auxiliary storage for chemicals, power generation systems, control rooms, and quarters for accommodation and office use (Amaechi et al. 2022). Hydrocarbon processing and storage equipment is installed on the topside after the completion of the platform structure and the equipment support foundation.

✉ Sezer Öztürk
sezer.ozturk@fsm.edu.tr

Ashraf Huseynli
eshref.huseynli98@gmail.com

Bülent Erkmen
bulent.erkmen@ozyegin.edu.tr

Ali Sari
asari@itu.edu.tr

[1] Offshore Structural Engineering, Saipem, Baku Ekonomic Zone, Karadag Raion, Azerbaijan

[2] Department of Civil Engineering, Fatih Sultan Mehmet Vakif University, Merkezefendi, Mevlevihane Rd., Topkapi Campus, Zeytinburnu, Istanbul 34015, Türkiye

[3] Department of Civil Engineering, Özyeğin University, Çekmeköy Campus Nişantepe District, Orman Street, Çekmeköy, İstanbul 34794, Türkiye

[4] Department of Civil Engineering, Istanbul Technical University, ITU Ayazaga Campus, Maslak, Istanbul 34469, Türkiye

Published online: 07 July 2025

Much of this equipment, including prefabricated facilities, is manufactured off-site and subsequently integrated on-site with the primary structural components of the platform topside (Chakrabarti 2005). Given the significant risks associated with potential equipment damage during a seismic event, including the possibility of hydrocarbon leakage and catastrophic consequences, the seismic evaluation of such equipment warrants rigorous investigation. A comprehensive understanding of the dynamic interactions between the topside facilities and the underlying platform structure is essential for ensuring the integrity and safety of these structures under seismic loading conditions. Maintaining the structural integrity and seismic resilience of offshore equipment is crucial for safe and efficient operations on offshore platforms.

In addition to seismic hazards, offshore platforms are exposed to a range of operational and environmental risks that necessitate robust risk management and reliability assessment strategies (Bhardwaj et al. 2020). While seismic risk is only one of many threats, methodologies developed for reliability and maintenance—such as those focused on minimizing downtime and ensuring operational safety (Ayele and Barabadi, 2016; Ratnayake 2018)—can also inform the evaluation of seismic resilience for topside equipment. Integrating these approaches helps to ensure that equipment remains functional and safe, even under extreme loading conditions.

Static seismic assessment methods have long been the most common approach for evaluating the seismic performance of structural components. However, to enhance the accuracy of seismic evaluations and to capture the complex dynamics of material and system behavior under seismic loads, nonlinear time-history analysis methods are increasingly employed for detailed seismic assessments of complex structural systems (Ozturk et al.,2023). Moreover, many contemporary design practices and construction codes require a specific number of time-history analyses. Structures such as offshore energy platforms, which support topside equipment containing flammable substances, require a more comprehensive and detailed assessment approach to ensure safety and structural integrity (Huseynli 2022).

Various methods and procedures exist for the seismic design of critical structural components. Several studies have investigated different approaches to assessing seismic effects on offshore structures (Visser 1997; El-Din and Kim 2015; Kee et al. 2023; Zafarjoo and Amirabadi 2023). The API Offshore Structure Standard (API RP-2EQ, 2014) provides comprehensive guidelines for the seismic design of offshore structures. This document is a modified adaptation of ISO 19901-2 (2004) and refers to two seismic design principles: extreme-level earthquakes (ELE), which utilize the ultimate limit state, and abnormal-level earthquakes (ALE), which utilize the accidental limit state. Offshore structures are classified based on their seismic risk category, determined by the seismic zone in which the structure is located and the exposure level of the structure (Table 1). The exposure level depends on the target annual probability of failure. The seismic zone is defined by the value for the 1 s horizontal spectral acceleration, $S_{a,\,map}(1.0)$, as given in Table 1. The design spectrum is constructed based on horizontal spectral acceleration values at 0.2 s ($S_{a,\,map}(0.2)$ and 1.0 s, which are obtained from generic seismic maps of spectral acceleration for offshore areas.

Table 1 Seismic zone identification table (API RP-2EQ, 2014)

$S_{a.map}$ (1.0)	<0.03 g	0.03 g to 0.10 g	0.11 g to 0.25 g	0.26 g to 0.45 g	>0.45 g
Seismic zone	0	1	2	3	4

The API guidelines explicitly state that topside equipment must be designed to withstand motions induced by ground shaking. The code emphasizes that topside motion can be significantly greater than that of the seabed and mandates the use of time-history analysis to assess topside deck movements. API RP-2FB (2016) also references various methodologies for explosion and fire assessment in offshore facilities.

Visser (1997) conducted a comprehensive assessment of the potential damage risks to offshore superstructures and facilities during extreme seismic events. He identified and classified several hazards associated with seismic activity, including damage to process equipment, rupture of riser pipelines, collapse of drilling rigs or cranes, failure of cantilever beam framing, collapse of accommodation modules, and failure of wells or conductors. To date, no critical seismic damage has been reported in offshore structures. However, Visser attributes this lack of reported damage not to superior structural design or performance, but rather to the absence of significant seismic activity affecting offshore structures. Due to the lack of earthquake-induced damage in offshore facilities, Visser recommends the application of event tree analysis to assess the risk of process equipment damage resulting from earthquakes with a 200-year return period. This event tree analysis was constructed using real-life scenarios from onshore facilities.

Pappa et al. (2013) conducted interdisciplinary research to develop detailed guidelines for the structural safety of steel liquid-storage tanks, pressure vessels, and piping systems subjected to seismic loading. Their research program included several phases: a comparative analysis of European and American industry standards, experimental testing to validate design assumptions, and finite element analysis (FEA) of the aforementioned facilities. To evaluate the structural integrity of offshore equipment—also known as pressure vessels—under horizontal loading,

nonlinear pushover analyses were performed on horizontal, vertical, and spherical-shaped vessels. The results indicated that the most critical stress concentrations occurred at the first shell course of the skirt and at the junction between the vessel and the skirt. It is also important to consider the influence of plate thickness on the seismic performance of such equipment. Research has shown that increasing plate thickness can enhance structural integrity and reduce stress concentrations under seismic loads (Hernandez et al. 2017; Das 2019). Furthermore, studies on spherical tanks have indicated that plate thickness is a key factor in enhancing structural integrity during earthquakes (Yang et al. 2011). Additionally, in the context of horizontal pressure vessels, thicker walls have been shown to improve seismic fragility (Korndörfer et al. 2017).

While the seismic performance of offshore platforms has been widely studied, most research has focused on the global structural response and dynamic analysis methods (Kim et al. 2017a, b; Tangtakabi et al. 2023). These studies provide a foundation for further investigation into the seismic behavior of integrated topside equipment. In addition, recent research has explored the behavior of offshore topside structures under special loads, such as impact and blast, and highlighted the potential of advanced materials for enhancing resilience (Pachaiappan and Chandrasekaran 2022). Structural health monitoring and durability assessment are also increasingly important for offshore platforms to ensure long-term safety and performance, and these techniques can support the evaluation of seismic effects on topside equipment (Murugan et al. 2023).

This study aims to address the significant gap in the literature regarding the seismic performance of topside equipment as an integrated part of offshore platforms. While previous research has primarily focused on the global seismic response of offshore structures or the behavior of similar equipment in onshore facilities, the unique dynamic interactions and risk factors associated with offshore topside equipment remain underexplored. In the present study, a comprehensive numerical investigation is conducted to evaluate the seismic response of various topside equipment installed on a representative fixed offshore platform. Rather than designing a new structure according to any specific standard, the analysis is performed on an existing offshore platform, reflecting real-world industry practice. For modeling details such as material properties and plastic strain thresholds, American standards were adopted to ensure methodological consistency and practical relevance. A finite element model of the platform, incorporating realistic physical properties, was developed using the ABAQUS general-purpose finite element software (Dassault, 2017), and a typical location on the topside layout was selected for the installation of different equipment types. The seismic performance of the equipment, modeled together with the platform, is assessed using advanced nonlinear time-history analysis, incorporating 22 high-magnitude earthquake records with three components each. Both coupled and uncoupled dynamic analyses are performed to capture the complex interactions between the platform and the equipment. The ground motion records include variations in peak ground acceleration, frequency content, duration, and both near-fault and far-fault effects, and are applied to the foundation of the jacket in three orthogonal directions. By integrating the equipment and platform into a unified numerical model and systematically evaluating their seismic response under realistic loading scenarios, this study provides new insights into the vulnerability and critical response parameters of topside equipment, offering practical recommendations for seismic design and risk mitigation, thereby making a novel contribution to the development of safer and more resilient offshore energy infrastructure.

2 Description of Offshore Platform and Equipment

A typical fixed offshore hydrocarbon production platform, which includes various equipment such as pressure vessels, accommodation facilities, and office buildings, consists of a jacket substructure that supports the topside, where oil and gas drilling and production facilities are located. The selected offshore platform features a pile arrangement measuring 30.48 m × 30.48 m, a topside layout of 15.23 m × 30.48 m, and a two-story superstructure with plan dimensions of 26.36 m × 53.15 m, as shown in Fig. 1. The overall height of the structure is 122.2 m, which includes a jacket height of 94.62 m and an inter-story height of 13.0 m. The total mass of the structure is 5,794.8 tons, comprising a topside mass of 4,672.2 tons and a jacket mass of 1,122.6 tons.

In the numerical model, the jacket, I-beam girders, columns, and truss elements were modeled using ASTM A36 steel, while the vessels and equipment were modeled with SA516 Grade 70 and SA537 Class 2 steel. To account for additional live loads and operational weights-such as piping, insulation, and equipment mass-the density of the structural elements was increased by 10%. This approach is consistent with practices commonly found in the literature and engineering applications, where a percentage increase in material density is used to represent permanent and live loads that are not explicitly modeled (Gerwick 2007; Pappa et al. 2013; Zafarjoo and Amirabadi 2023). A summary of the main I-beam and tubular steel sections, along with their dimensions, is provided in Tables 2 and 3, respectively.

For offshore equipment, five pressure vessel-type units commonly used in the offshore hydrocarbon industry were

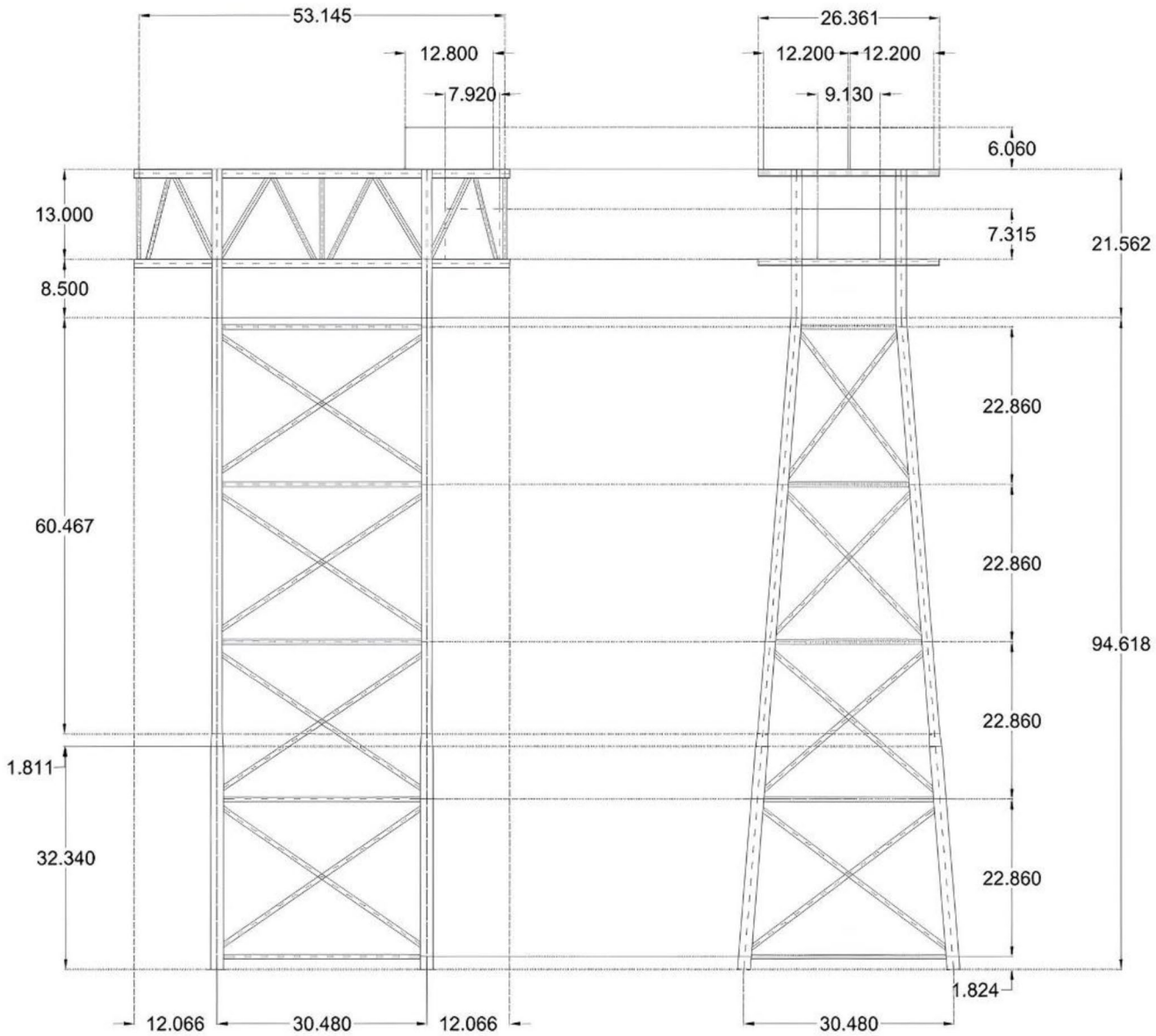

Fig. 1 Front and side elevations of the platform (all dimensions in m)

Table 2 List of I-beam and circular tubular sections

Element name	h (m)	b (m)	t_w (m)	t_f (m)	
Girders	1.27	0.56	0.03	0.04	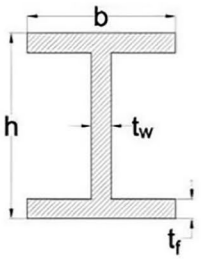
Primary beams	0.93	0.42	0.02	0.04	
Secondary beams	0.36	0.17	0.01	0.01	

Table 3 List of pipe sections used in the structure

Element name	d (m)	t (m)
Jacket columns' lower part	1.83	0.04
Jacket columns' upper part	1.53	0.04
Jacket trusses	0.66	0.014
Topside columns	1.53	0.04
Topside truss elements #1	0.76	0.038
Topside truss elements #2	0.61	0.02

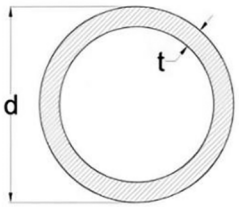

considered for the platform. These selected vessels store flammable substances, making them critical components due to the associated risks of fire and explosion-induced structural failures. Typically, most offshore equipment is designed to meet specific project requirements rather than adhering to standardized dimensions. Consequently, the physical dimensions of the vessels were tailored to fit the chosen offshore platform.

Vessels are generally classified into two primary categories based on their shape and method of support on the platform: vertical vessels (VE), which utilize skirts or support legs, and horizontal vessels (HE), which employ saddle supports. This study examines two vertical vessels (VE1 and VE2) with skirts: one slender vessel with a height-to-diameter ratio (H/D) of 11, and another with a ratio of 3. The H/D ratio significantly influences the dynamic response of vessels during seismic events. Taller, slender tanks typically experience higher inertial forces, leading to increased swaying or oscillation compared to shorter, wider tanks (with a low H/D ratio). Additionally, vessels with high H/D ratios are more prone to overturning or structural failure during seismic incidents, as they exhibit large overturning moments and greater demands on the base connections. A third vertical vessel (VE3) with support legs, possessing an H/D ratio of 2.25, was also considered to evaluate the impact of base support on the behavior of vertical vessels.

Saddle support systems are widely used for horizontal pressure vessels due to their effectiveness in providing stable and reliable support. A typical saddle support consists of two semi-cylindrical (half-round) structures that cradle the vessel and are usually welded or bolted to its underside. These supports are strategically positioned to distribute the vessel's weight and the effects of internal pressure evenly to the supporting structure or foundation, thereby minimizing local stress concentrations. The placement of saddle supports is a critical design consideration. If the supports are positioned too close to the vessel ends, the central span may experience excessive bending and deflection. Conversely, if the supports are placed too close together near the center, the cantilevered ends may be subjected to high stresses and potential uplift, especially under seismic or dynamic loading. Therefore, the optimal location of saddle supports is typically determined through structural analysis, taking into account the vessel's length, diameter, wall thickness, and operational loads, as well as thermal expansion and contraction effects. Saddle supports are also designed to accommodate thermal movements, which are common in pressure vessels due to temperature fluctuations during operation. This is often achieved by allowing one support to act as a fixed point (anchored) while the other permits sliding, thus preventing excessive thermal stresses and maintaining the vessel's structural integrity. In this study, two horizontal vessels (HE1 and HE2) with saddle supports are analyzed, primarily distinguished by the location of their supports. In one vessel, the supports are positioned near the ends, while in the other, the supports are placed closer together near the center. This configuration allows for the investigation of how support placement influences the vessel's dynamic response and stress distribution under seismic loading. Figure 2 presents the topside equipment considered in this study.

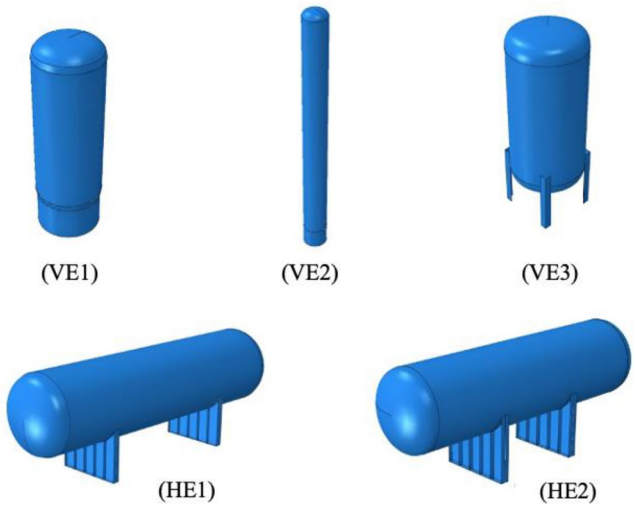

Fig. 2 Configuration of topside equipment - vertical vessels with skirt (VE1 and VE2), vertical vessels with support legs (VE3), and horizontal vessels with saddles (HE1 and HE2)

Fig. 3 FEA model of the offshore platform

Table 4 Mechanical properties of the materials in the model

Material type	Yield strength (MPa)	Tensile strength (MPa)	Elongation in 5 cm
SA537 Class 2	413	550–690	% 22
SA516 Grade 70	262	480–620	% 21
A36	248	400–550	% 21

3 Platform and Equipment Computational Model

The nonlinear time-history earthquake analysis of the platform and equipment was performed using the general-purpose finite element code ABAQUS (2017), selected for its computational efficiency and stability in nonlinear time-history analyses. The model, illustrated in Fig. 3, includes the jacket, two decks, and various equipment. All structural elements, including the platform jacket, decks, living quarters, and equipment, were modeled using S4R shell elements, which are 4-node general-purpose shell elements with reduced integration. This element type is well-suited for conducting large strain analyses on both thin and thick shells. The structural components of the platform were modeled using ASTM A36 steel material properties. However, the pressurized vessels were modeled using standard steel grades, specifically ASTM SA516 Grade 70 and ASME SA537 Class 2, which are commonly used for pressurized equipment applications. Elastic-perfectly plastic material properties were assigned to all components, as summarized in Table 4. To account for additional permanent and operational loads-such as piping, insulation, and equipment mass-the density of the structural elements was increased by 10%. This approach is consistent with practices in the literature and ensures a more realistic representation of the total mass and dynamic response of the offshore platform under seismic loading.

Table 5 Platform and equipment nominal mesh size

Structural elements & Equipment	Nominal mesh size (m)
Jacket columns	2.0
Jacket truss elements	0.25
Rest of platform (columns, girders, and beams)	0.20
HE1 saddles & walls	0.13
HE2 saddles & walls	0.22
VE1 skirt & walls	0.10
VE2 skirt & walls	0.10
VE3 support legs &walls	0.04

The member end connections were modeled using node-to-node tie constraints. This approach enables the use of varying nominal mesh sizes for different elements, effectively minimizing mesh distortion in congested areas or regions with complex connections. Due to the complexity of the developed model, different nominal mesh sizes were assigned to various parts of the structure, as summarized in Table 5. The mesh size for each component was selected based on geometric complexity, expected stress concentrations, and material properties. A typical nominal mesh size of 0.20 m was used for structural elements such as girders, beams, truss elements, and columns. A larger mesh size was adopted for jacket columns, while a much finer mesh was applied to vessel equipment to ensure that the element size did not exceed one-tenth of the smallest characteristic length of the geometry. This meshing strategy ensures adequate resolution of stress gradients and accurate capture

of local effects, particularly in areas with high stress concentrations or complex geometries.

In the offshore structure model, dead loads were calculated based on the self-weight of all elements and components. To account for additional dead loads not explicitly represented in the model-such as piping, insulation, and equipment mass-the density of the jacket elements was increased by 10%. This approach ensures a more realistic representation of the total mass and dynamic response of the structure. The strong ground motions selected for the finite element analyses are described in the following section.

4 Strong Ground Motion Selection Procedure

Nonlinear time history analyses of the platform were performed using all three components of recorded accelerograms from 22 natural strong ground motions. Both horizontal and vertical components were included to properly capture the effects of vertical excitation, torsional effects due to nonuniform mass distribution, and the interaction of these components on the seismic performance of the platform and its equipment. The records were selected from the Pacific Earthquake Engineering Research (PEER 2022) Center NGA-West2 database. A variety of selection criteria, identified as critical by various scientific sources, were employed to develop a diverse and comprehensive ground motion database. One key ground motion characteristic considered was the near-fault effect, which occurs in regions with short fault distances. This effect arises when the slip direction aligns with the rupture direction, causing the fault rupture to propagate toward the surface. Near-fault ground motions are distinguished by distinct displacement and velocity pulses that transmit substantial energy to structures (Ozturk and Sari, 2024). There are two primary types of near-fault effects: forward directivity and fling-step effects. Forward directivity is characterized by a bidirectional velocity pulse that leads to corresponding displacement pulses, while the fling-step effect is identified by a unidirectional velocity pulse accompanied by permanent ground displacement. Research has shown that near-fault ground motions induce higher displacement demands in structures with longer natural periods compared to other ground motion types (Kalkan and Kunnath 2006; Sehhati et al. 2011; Hamidi et al., 2019; Alothman et al. 2021). Considering these critical characteristics, ten near-fault ground motion records were selected for the time-history analyses.

The peak ground acceleration (PGA) to peak ground velocity (PGV) ratio is another key criterion that has been widely recognized in the literature as a significant parameter for evaluating ground motions. Sawada et al. (1992) investigated the relationship between PGA/PGV ratios, spectral characteristics, and the duration of earthquake motions using a dataset of 148 acceleration records. Their findings indicate that the PGA/PGV ratio is an important indicator of an earthquake's spectral properties and duration; specifically, a lower PGA/PGV ratio is associated with a smaller dominant frequency and a longer period. Additionally, their results demonstrated a negative correlation between the PGA/PGV ratio and factors such as earthquake magnitude, epicentral distance, and the site's dominant period. To ensure a comprehensive representation of ground motion characteristics, a diverse range of PGA/PGV ratios was considered in the ground motion selection process.

Earthquake magnitude is another widely utilized parameter for quantifying seismic events, defined as the logarithmic measure of the total seismic moment released at the earthquake source. Among various parameters, earthquake magnitude directly influences the frequency content characteristics of ground motion. Several scalar parameters are used to characterize these frequency content aspects, including the mean period (T_m) and the average spectral period (T_{avg}), which are related to the low-frequency content, while the spectral predominant period (T_0) pertains to the high-frequency content. Rathje et al. (2004) empirically examined the relationship between frequency content parameters and earthquake magnitude using a comprehensive ground motion database with consistent rupture distance and site conditions. Their results revealed significant correlations between earthquake magnitude and frequency content parameters, suggesting that higher magnitudes enhance the structural response to ground motions. Consequently, all ground motion records selected for this study have magnitudes greater than 6.0 to ensure the inclusion of strong seismic events.

The geotechnical profile is another critical parameter that directly influences ground motions by affecting both their amplitudes and response spectra. However, using the soil profile as a selection criterion can significantly limit the number of available ground motion records. Boomer and Scott (2000) observed that incorporating soil profile, along with magnitude and rupture distance, as a selection criterion substantially reduced the dataset size (PEER 2022). They suggested that, in certain cases, it may be necessary to neglect the soil profile as a selection parameter. In this study, ground motion records with various soil characteristics were utilized without focusing on the geotechnical properties of a specific site.

In addition, the duration of ground motion is another critical parameter for selection, as longer-duration earthquakes transfer more energy to the structure. To ensure a worst-case scenario, the minimum duration of the selected ground motions in this study was set at 15 s. Due to the limited

availability of historical ground motion records, amplitude scaling was applied to the existing records. To evaluate the structural response under elevated ground acceleration values, the acceleration records were multiplied by specific scaling factors. In this study, four earthquake records (Duzce - Bolu, Loma Prieta - WAHO, Kobe - Nishi-Akashi, Imperial Valley - El Centro Array #8) were each scaled twice to ensure that the time-history records covered a range of PGA values from 0.9 g to 1.7 g. Based on the selection criteria outlined above, the ground motion database presented in Table 6 was established. In this study, the primary objective was to investigate the general seismic response of offshore platforms and their equipment under a wide range of earthquake intensities and ground motion characteristics. Therefore, the analyses were not tailored to a specific geographic region or design code, and no target design spectrum was selected for scaling the ground motion records. Instead, a suite of real earthquake records with varying peak ground acceleration (PGA) values and frequency content was used to provide a comprehensive assessment of structural performance. This approach is consistent with previous studies in the literature that aim to evaluate the general behavior of offshore structures under diverse seismic scenarios, rather than focusing on code-based or site-specific design requirements (e.g., Kalkan and Kunnath 2006; Rathje et al. 2004).

5 Dynamic Analyses

The previously selected three-component ground motions were applied to the finite element analysis (FEA) model as illustrated in Fig. 4. The predominant horizontal component (EQZ) was applied along the weaker axis of the structure, while the secondary horizontal component (EQX) was applied in the orthogonal horizontal direction. The vertical component (EQY) was applied in the vertical direction, as shown in Fig. 4.

The ground motions were applied to the four platform supports, as shown in Fig. 5, by imposing the earthquake acceleration histories as boundary conditions in three orthogonal directions. In a preceding static analysis step, gravity loads were applied while the support boundary conditions were fixed in all degrees of freedom. During the subsequent implicit dynamic analysis step, the earthquake accelerations were introduced by releasing the displacement degrees of freedom in the directions of the earthquake components and applying the corresponding acceleration histories as base excitations. This approach allows the supports to respond dynamically to the imposed ground motions, accurately simulating the seismic loading conditions.

The seismic design of equipment mounted on floors is typically performed using floor response spectra (FRS) to determine appropriate anchoring methods and support configurations that mitigate seismic-induced displacements and forces. However, the FRS approach may overlook

Table 6 Ground motion database

EQ ID	Name	Station	Year	M_w	R_{jb} (km)	PGA (g)	PGV (cm/s)	PGA/PGV	Duration (s)	Scaling	T_p (s)
GM01*	Landers	Lucerne	1992	7.3	2.2	0.7	133.5	5.3	25	-	0.08
GM02*	L.-Prieta	Corralitos	1989	6.9	0.2	0.6	56.0	11.3	25	-	0.3
GM03*	Kobe	KJMA	1995	6.9	0.9	0.8	91.1	9.0	24	-	0.36
GM04*	Northridge	Rinaldi	1994	6.7	0.0	0.9	148.1	5.8	16	-	0.7
GM05*	Chi-Chi	TCU075	1999	7.6	0.9	0.3	109.6	3.0	36	-	0.36
GM06*	Loma-Prieta	LGPC	1989	6.9	0.0	0.6	96.1	5.8	20	-	0.7
GM07*	Kocaeli	Yarimca	1999	7.5	1.4	0.2	69.7	2.8	24	-	0.52
GM08*	Erzincan	Erzincan	1992	6.7	0.0	0.4	107.1	3.5	15	-	0.96
GM09*	Chi-Chi	TCU068	1999	7.6	0.0	0.5	240.6	2.1	29	-	0.42
GM10	L.-Prieta	S.-Aloha ave.	1989	6.9	7.6	0.3	46.0	7.0	15	-	0.2
GM11	Duzce	Duzce	1999	7.1	0.0	0.5	84.1	6.0	26	-	0.22
GM12	Chi-Chi	CHY080	1999	7.6	0.1	0.9	92.7	9.1	34	-	0.84
GM13	S. Hills-02	El C. Imp.	1987	6.5	18.2	0.4	48.1	7.3	40	-	0.22
GM14	V. Mexico	Cerro Prieto	1980	6.3	13.8	0.6	33.6	18.8	15	-	0.06
GM15	Northridge	LA-N W.	1994	6.7	23.4	0.3	24.2	13.5	25	-	0.32
GM16	Chi-Chi	TCU079	1999	7.6	0.0	0.6	70.5	8.2	50	-	1.98
GM17	M. Hill	C. Lake Dam	1984	6.2	0.2	1.3	78.4	16.3	15	-	0.3
GM18	S. Fernando	P. Dam	1971	6.6	0.0	1.2	114.5	10.4	15	-	0.42
GM19*	I. Valley-06	El C. A. #8	1979	6.5	3.9	1.2	109.0	11.0	25	x2	1.06
GM20	L.-Prieta	WAHO	1989	6.9	11.0	1.3	76.2	16.8	27	x2	0.14
GM21	Kobe	Nishi-Akashi	1995	6.9	7.1	1.0	93.7	10.1	16	x2	0.24
GM22	Tabas, Iran	Tabas	1978	7.4	1.8	1.7	246.6	6.9	27	x2	0.2

(*) ground motions with near fault effects

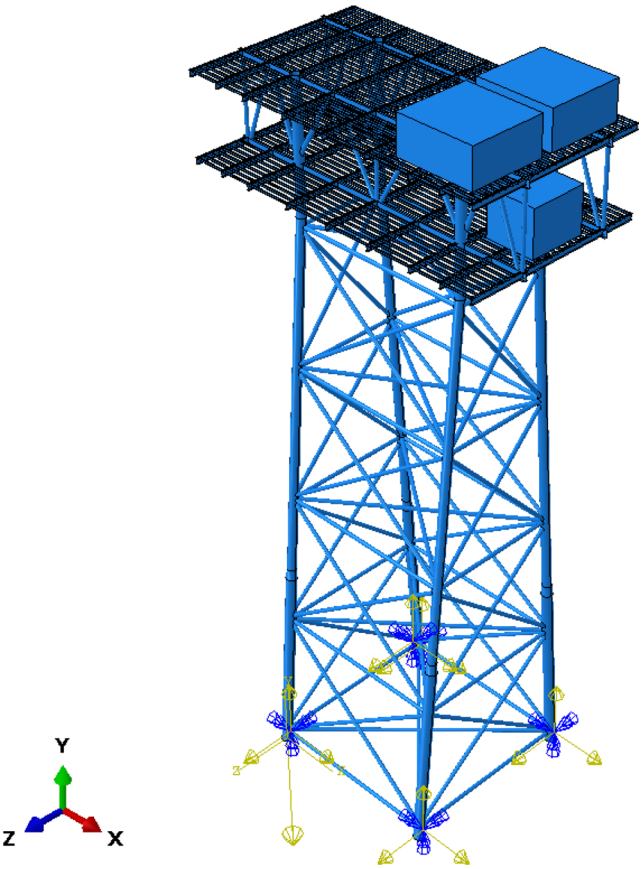

Fig. 4 Orientation of ground motion components

significant complexities such as local modal coupling, torsional irregularities, and the nonlinear behavior of materials, potentially resulting in conservative estimates of the seismic demands on the equipment. In contrast, full finite element modeling integrates both the primary structure, including the floors, and the attached equipment, effectively capturing complex interactions such as nonlinear effects, multiple vibrational modes, torsional responses, and a more accurate representation of seismic mass distribution. Nevertheless, implementing full finite element modeling requires substantial computational resources and intricate model development. As a result, two seismic analysis approaches were employed for the equipment on the platform, as illustrated in Fig. 6. The first approach, termed uncoupled equipment analysis, utilizes the computed seismic displacement histories at the upper deck column, which is assumed to be sufficiently rigid to follow the deck's motion. The seismic displacement histories from the column reference node (shown in Fig. 5) are adopted as the input for the equipment supports. This method reduces computational costs while enabling the assessment of the seismic performance of horizontal equipment, with supports aligned both along and perpendicular to the direction of the principal earthquake component, as shown in Fig. 6. Importantly, this approach eliminates the need to rerun the seismic model of the platform for different equipment layouts.

The second approach, depicted in Fig. 6c, involves developing a full finite element model of the platform and equipment for a selected set of earthquake ground motions that impose the highest demand on the equipment, as identified

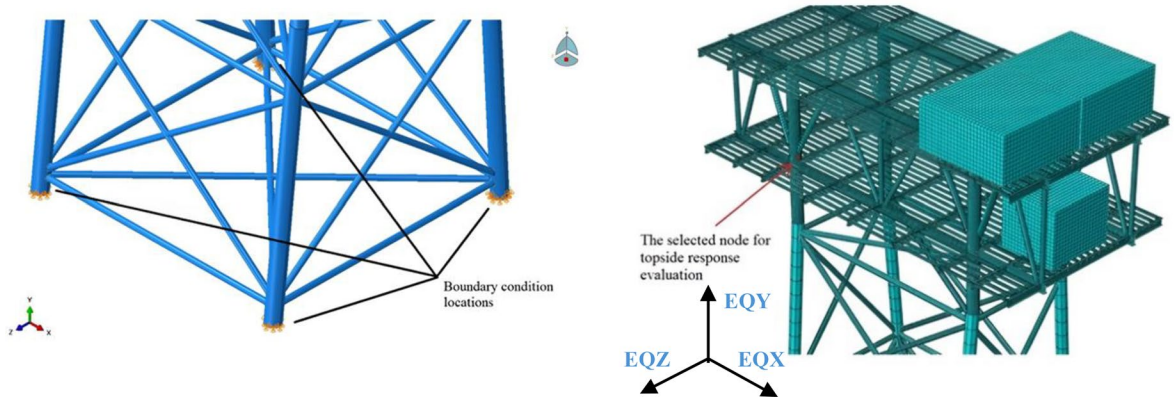

Fig. 5 Boundary condition and reference node for uncoupled equipment analysis

Fig. 6 Equipment support orientation: (**a**) aligned, (**b**) perpendicular to the significant EQ component (uncoupled), and (**c**) perpendicular (coupled)

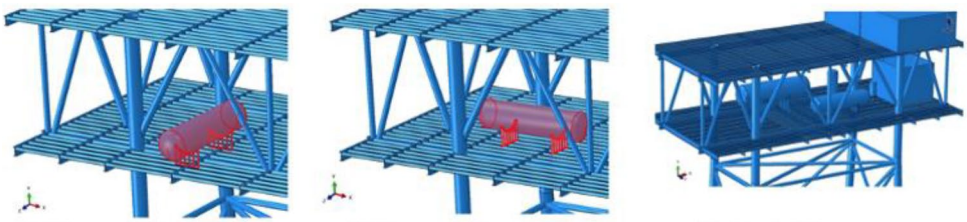

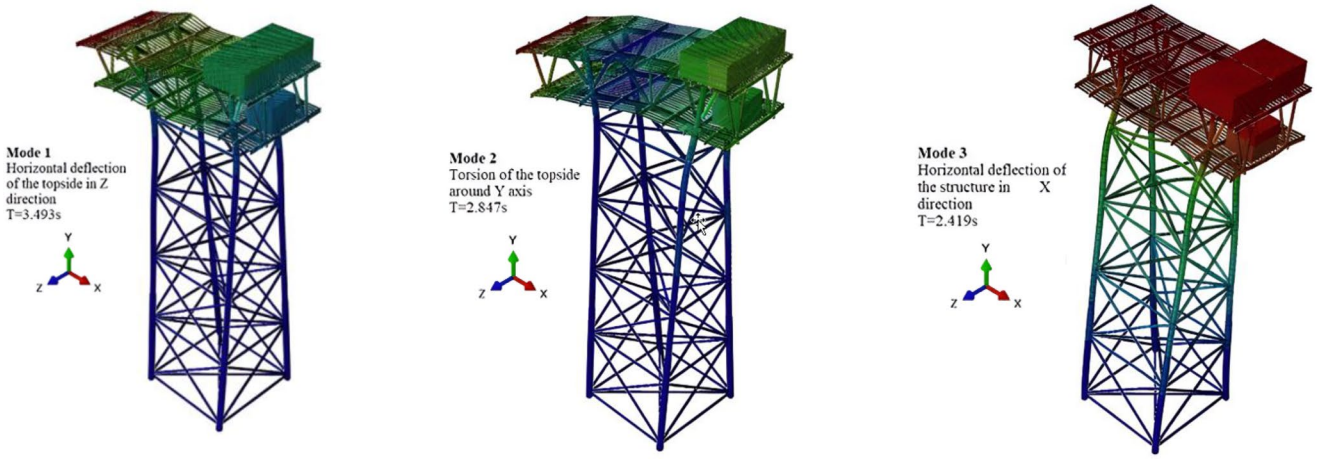

Fig. 7 Modal analysis results of the platform model

Table 7 Platform peak displacements

EQ ID	Max. δ (m)
GM01*	1.459
GM02*	0.124
GM03*	0.186
GM04*	0.281
GM05*	1.509
GM06*	0.403
GM07*	0.582
GM08*	0.257
GM09*	>2
GM10	0.277
GM11	0.449
GM12	0.222
GM13	0.261
GM14	0.079
GM15	0.084
GM16	0.170
GM17	0.105
GM18	0.321
GM19*	0.869
GM20	0.314
GM21	0.184
GM22	>2
Average	0.552

through the uncoupled seismic analysis. This method facilitates a direct comparison of various seismic analysis techniques and their effects on the seismic performance of large offshore equipment.

6 Results and Discussions

6.1 Offshore Platform

Modal analysis of the platform was performed to identify the mode shapes and their corresponding vibration periods. Figure 7 presents the first three dominant modes, with periods of 3.49 s, 2.85 s, and 2.42 s, respectively. The first mode corresponds to horizontal deflection in the Z-direction, the second mode represents torsional deformation, and the third mode corresponds to horizontal deflection in the X-direction. The pronounced torsional mode primarily results from the unsymmetrical distribution of seismic mass, caused by the office and living quarters being located at one end of the platform.

The time-history analysis results of the platform indicate significant displacements, material yielding in the main jacket columns just below the lower deck level, and structural damage. This damage is primarily attributed to deflection in the Z-direction, which corresponds to the first mode shape, as illustrated in Fig. 7. These findings suggest that the seismic performance of the platform could be improved by incorporating additional braces between the lower deck and the columns. Table 7 summarizes the maximum relative displacements (δ) of the platform in response to each selected ground motion. The average maximum peak displacement value of the platform is 0.552 m. Notably, permanent deformation exceeded 1.0 m in the upper section of the platform during ground motions GM01* and GM05*, both of which are near-fault events. Furthermore, structural collapse was observed under near-fault ground motion GM09* and ground motion GM 22, due to significant deformation of the platform, as illustrated in Fig. 8. The * symbols indicate earthquake records that include near-fault effects.

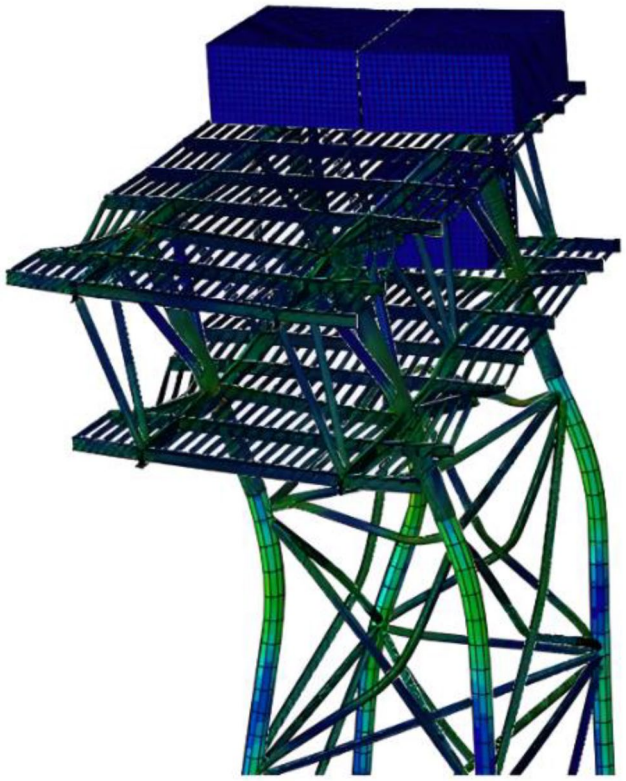

Fig. 8 Failure moment of the platform under ground motion GM22

Figure 9 illustrates the relationships between platform peak displacement and key ground motion parameters—namely PGA, PGV, the PGA/PGV ratio—based on 22 ground motion records. The results demonstrate that PGV serves as the most reliable predictor of platform peak displacement, corroborating previous findings (Katsanos et al. 2010; Gazi and Alhan 2019). Notably, all observed platform failure cases are associated with high PGV values, suggesting that velocity-dominated ground motions exert a more significant influence on large structural displacements. This observation further underscores the critical importance of PGV in evaluating ground deformation risks. Consequently, the findings emphasize the necessity of prioritizing PGV over PGA in seismic hazard assessments and structural design considerations.

6.2 Equipment Seismic Performance-Uncoupled

The uncoupled equipment seismic analysis utilizes the deck column seismic displacement histories as input boundary conditions for the equipment supports. According to Pappa et al. (2013), two distinct plastic strain distributions can develop at horizontal equipment saddle supports, depending on the direction of the horizontal loading. Specifically, one distribution occurs when the load is parallel to the support line, and another when it is perpendicular. Therefore,

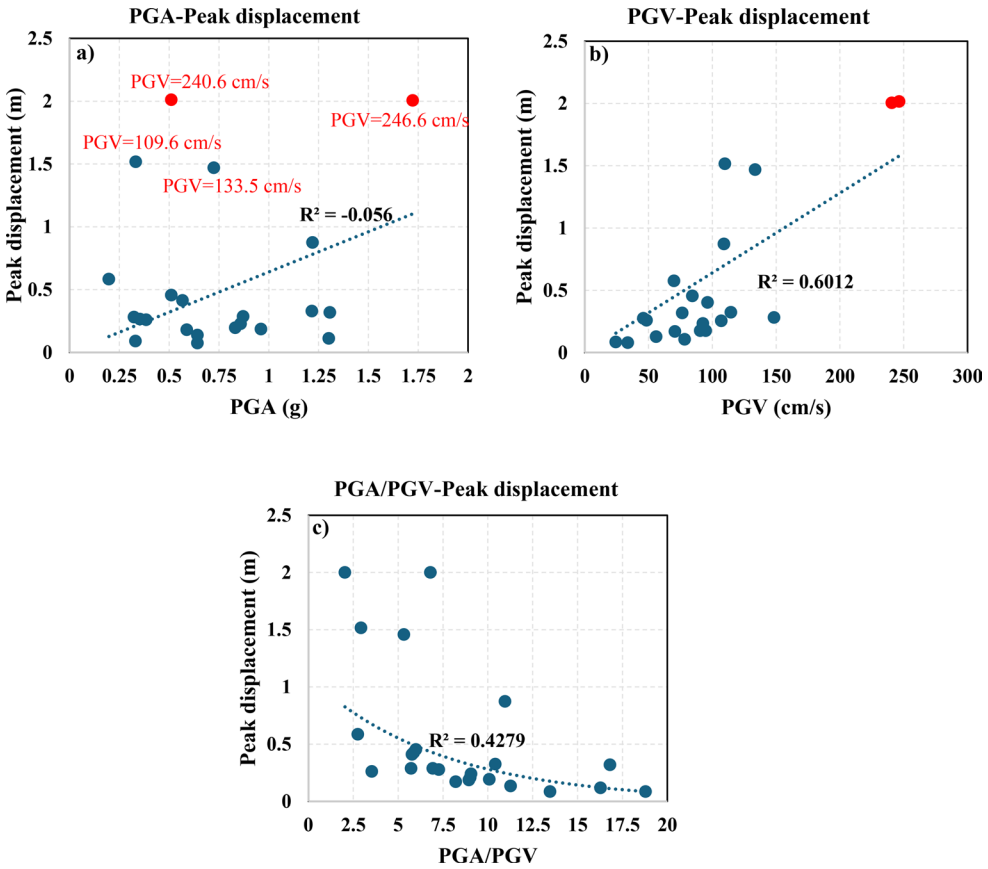

Fig. 9 Relationship between platform peak displacement and ground motion parameters (**a**) PGA, (**b**) PGV, and (**c**) PGA/PGV

two equipment layouts are considered: Layout-A, where the equipment support line aligns with the direction of the significant earthquake component, and Layout-B, where the support line is perpendicular to this direction, as illustrated in Fig. 6.

Modal analyses are performed for both horizontal and vertical equipment to determine their natural vibration modes, as shown in Fig. 10. These modes are compared with the platform's natural frequencies to ensure sufficient frequency separation and minimize resonance effects. A common engineering practice is to maintain at least a 20–30% frequency

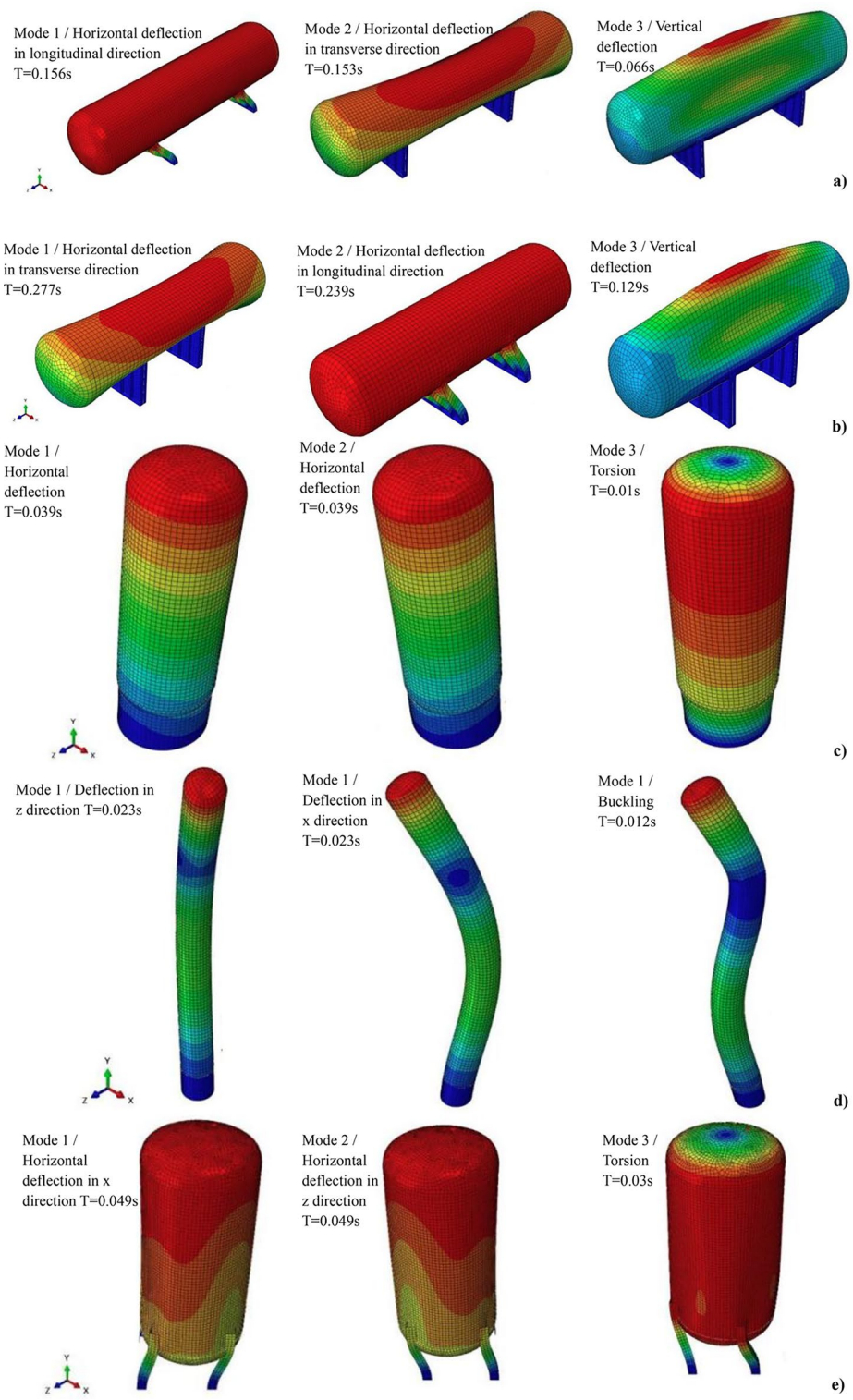

Fig. 10 Mode shapes and vibration periods of equipment **a**) HE1, **b**) HE2, **c**) VE1, **d**) VE2, and **e**) VE3

Table 8 Summary of equivalent plastic strains for equipment-uncoupled seismic analysis

EQ ID	Equivalent plastic strain PEEQ (%)			
	HE1	HE2	VE1	VE3
GM01	0.044 (0.004)	0.0479 (0.075)	0.0810	0.0223
GM02	0.31 (0.079)	0.0262 (0.23)	0.0297	0.0096
GM03	0.303 (0.681)	0.003 (0.434)	0.0464	0.2
GM04	0.0026 (0.0053)	0.0024 (0.0023)	0.0468	0.0188
GM05	0.0023 (0.0036)	0.0306 (0.0023)	Collapse	0.0417
GM06	0.0743 (0.11)	0.0023 (0.17)	0.0365	0.1456
GM07	0.0030 (0.0054)	0.0516 (0.10)	0.0873	0.0346
GM08	0.00 (0.0034)	0.00 (0.0025)	0.0159	0
GM10	0.00 (0.0030)	0.00 (0.0031)	0	0
GM11	0.0910 (0.368)	0.002 (0.0046)	0.0543	0.0052
GM12	0.0696 (0.411)	0.3409 (0.32)	0.1622	0.0438
GM13	0.143 (0.124)	0.00 (0.0062)	0.1496	0.0418
GM14	0.0001 (0.0005)	0.0004 (0.08)	0.0001	0
GM15	0.001 (0.0007)	0.0002 (0.0032)	0	0.0009
GM16	0.284 (0.112)	0.0021 (0.0073)	0.1091	0.0154
GM17	0.001 (0.007)	0.0030 (0.52)	0.024	0
GM18	0.002 (0.0287)	0.0260 (0.25)	0.087	0.0023
GM19	0.244 (0.302)	0.0018 (0.082)	0.1545	0.0016
GM20	0.398 (0.294)	0.2351 (1.27)	0.1556	0.3511
GM21	0.014 (0.083)	0.0611 (0.94)	0.0695	0.0974
Average	0.099 (0.131)	0.0418 (0.2251)	0.0655	0.0561

Values within parentheses are for horizontal equipment layout-B

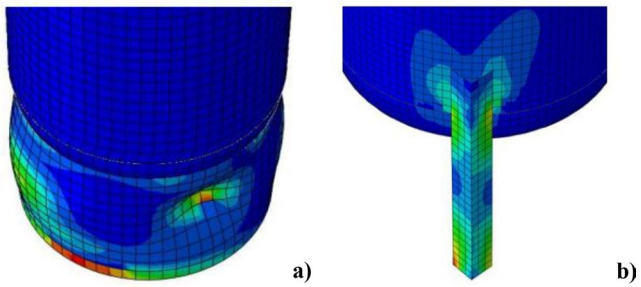

Fig. 11 Common plastic strain distribution on the **a**) VE1, **b**) VE3 vertical vessels

separation between the equipment and the supporting floor to avoid resonance. In this study, the first three fundamental natural frequencies of the vertical equipment (VE1, VE2, and VE3) range from 25.64 to 100 Hz, while the horizontal equipment frequencies span from 6.41 to 15.15 Hz. These vibration frequencies are well separated from the platform's natural frequencies, with a minimum frequency separation of 88% (calculated as the difference between the closest equipment and platform frequencies, divided by the platform frequency). This large separation ensures that no significant amplification of equipment dynamic response (e.g., displacement or acceleration) occurs during seismic events.

Table 8 Presents the maximum plastic strain values occurring at the saddle supports for the application of the critical ground motion components in both horizontal directions.

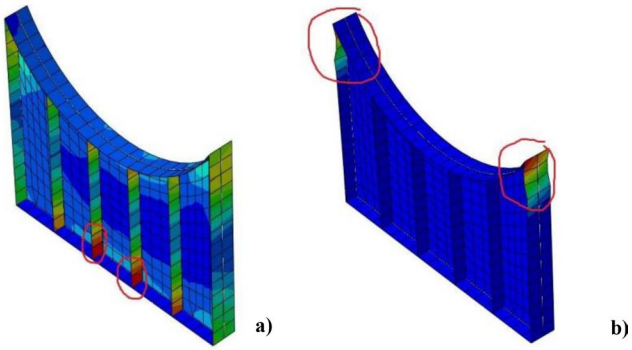

Fig. 12 The average plastic strain distribution occurring in saddles during impact in; **a**) longitudinal direction **b**) transverse direction

Due to the boundary conditions, the VE2 model performs as a rigid beam under dynamic impacts, and any failure and plasticity formation is not observed from the analysis results.

Figure 11 shows the PEEQ contours of vertical vessels under GM05, where the strain values are close to the average PEEQ values across all considered ground motions. As expected, material yielding and damage occur near the base connections for VE1 and VE3. For VE3, which has support legs, the legs experience material yielding, while the leg-vessel connection undergoes localized yielding.

The results show the difference in plastic strain distribution while applying the critical horizontal component of top-side motion in each direction shown in Fig. 12. The regions exposing to the biggest strain values harmonize with Pappa et al. study as seen from the figures.

The relationship between the maximum equivalent plastic strain (PEEQ) in both vertical and horizontal vessels and key ground motion parameters was investigated. Fig. 13 shows this relationship for HE1 with Layout-A. Similar trends were observed for Layout-B and horizontal equipment; therefore, their graphs are not included.

As seen in these graphs, peak ground acceleration (PGA) values above 0.5 g show the formation of critical plasticity percentages in the joints. The presence of lower damage levels generated by ground motions with PGA values greater than 0.5 g is explained as a result of the duration of the ground motion, since ground motions lasting over approximately 20 s appear to independently increase plastic strain formation. The peak plastic strain values resulting from the application of the critical ground motion components in the longitudinal and transverse directions for each ground motion are presented in Fig. 14.

It is observed that transverse loading causes more damage to the saddle supports, whereas the longitudinal oscillation predominantly appears in the first mode of free vibration. The saddle supports are designed with multiple ribs to resist longitudinal impacts, which, regardless of the mode shape

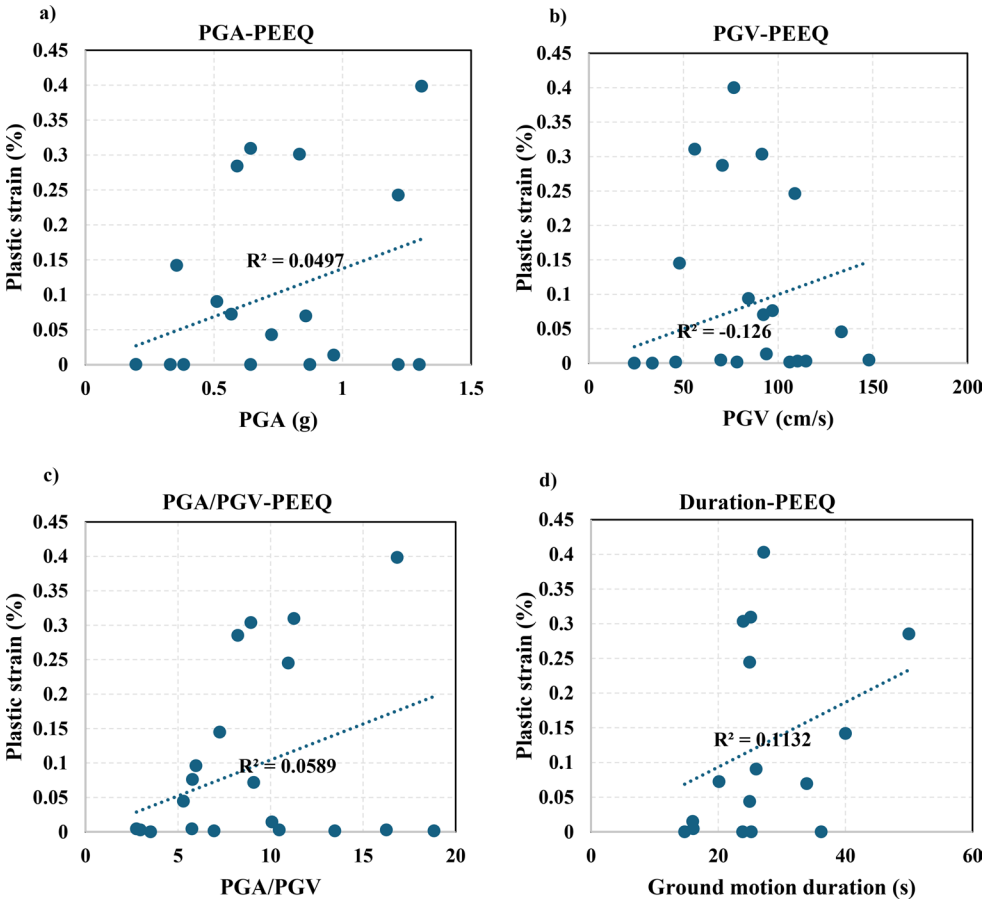

Fig. 13 Relationship between HE1 maximum PEEQ values and ground motion parameters **a**) PGA, **b**) PGV, **c**) PGA/PGV, and **d**) EQ duration

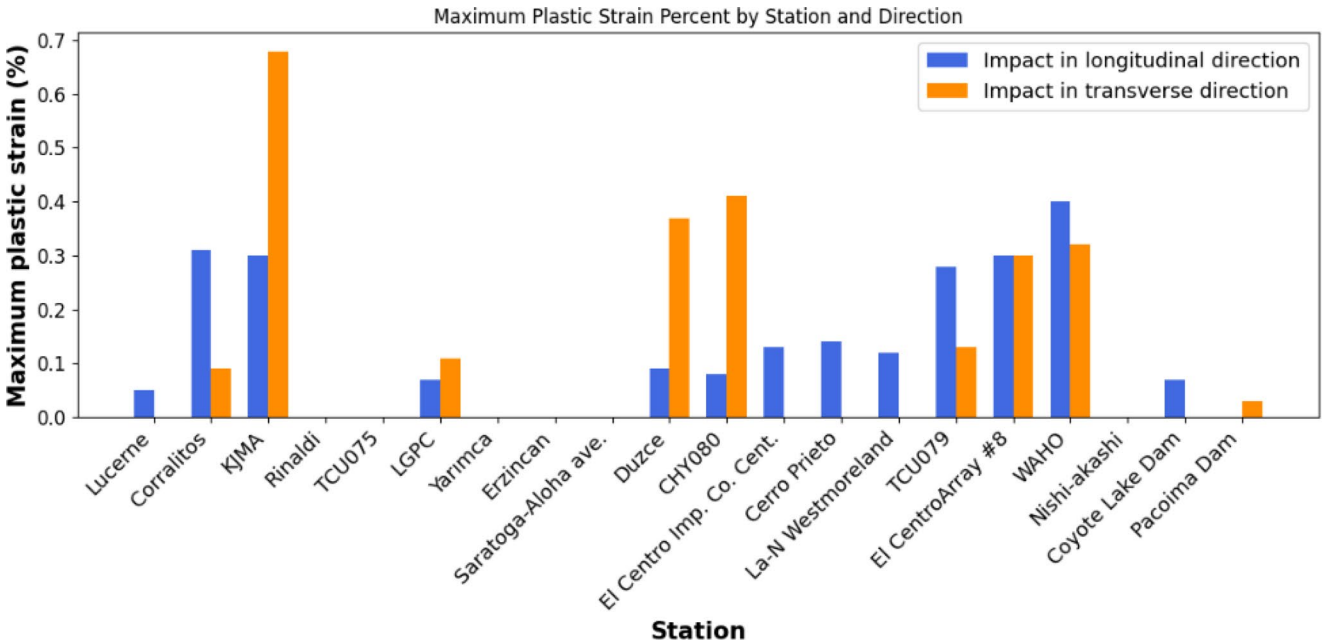

Fig. 14 Maximum plastic strain percentage by each ground motion for longitudinal and transverse impact

distribution, enhances the elastic behavior of the horizontal vessels in the longitudinal direction. The amount of plastic strain differs for each direction of horizontal impact. To mitigate this discrepancy and ensure that the saddles perform equally under both loading directions, the cross-sectional areas of the outer ribs have been increased by a factor proportional to the ratio of plastic strains observed in the two directions. The results indicate that this approach is effective, and that increasing the cross-sectional areas of the outer ribs by a factor of 2 to 5 can provide a practical solution for optimizing saddle support design.

Near-fault ground motion records, which are characterized by displacement and velocity pulses, have been shown to independently induce material plasticity and fracture in structures. To assess the validity of this phenomenon within the context of the present study, time history analyses were performed by applying near-fault ground motion records along the weak axis of the platform model. The resulting plastic strain development in the four-rib saddle supports is illustrated in Fig. 15.

The analysis results demonstrate that the displacement impulse generated by the forward directivity effect influences the development of plastic strain at the vessel support, regardless of vessel geometry, support type, or ground motion parameters. Furthermore, the results indicate that the vertical vessel #1 model is consistently affected by displacement impulses. This can be attributed to the dynamic response characteristics of objects with shorter vibration periods, which tend to fail together with the main structure during seismic excitation and therefore do not exhibit independent seismic performance.

6.3 Equipment Seismic Performance-Coupled

To evaluate the differences between uncoupled and coupled analyses, the three most destructive ground motions—GM03, GM04, and GM19—were selected. The coupled model, in which both vertical and horizontal equipment are installed on the lower deck of the platform, is illustrated in Fig. 6. The horizontal equipment was arranged according to Layout-B, as uncoupled seismic analyses indicated that this configuration is more critical than Layout-A. Fig. 16 presents the plastic strain (PEEQ) contours for horizontal equipment HE1 under GM04 excitation. The results reveal that both models predict similar strain distributions and potential damage locations. However, the maximum PEEQ

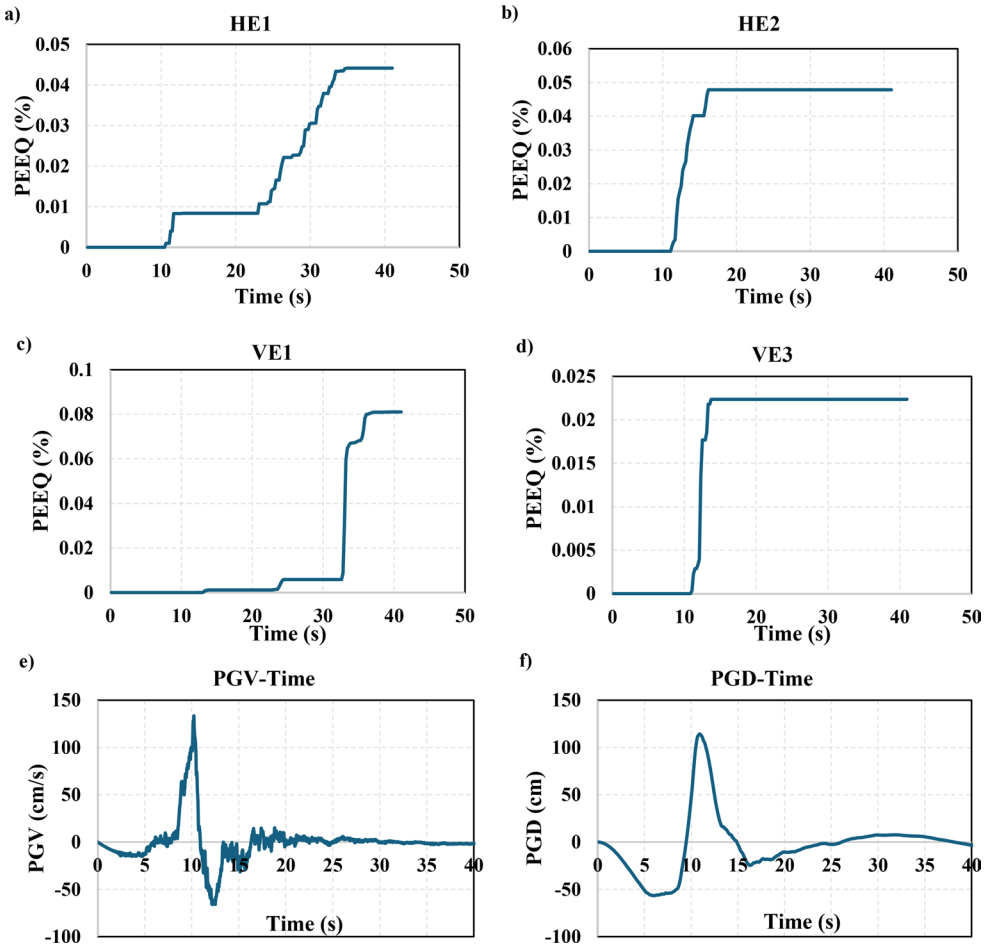

Fig. 15 The effect of displacement pulse on the damage formation in vessels during analysis under GM01, equivalent plastic strain time histories for equipment **a**) HE1, **b**) HE2, **c**) VE1, **d**) VE3, and **e**) PGV, **f**) PGD time histories for GM01

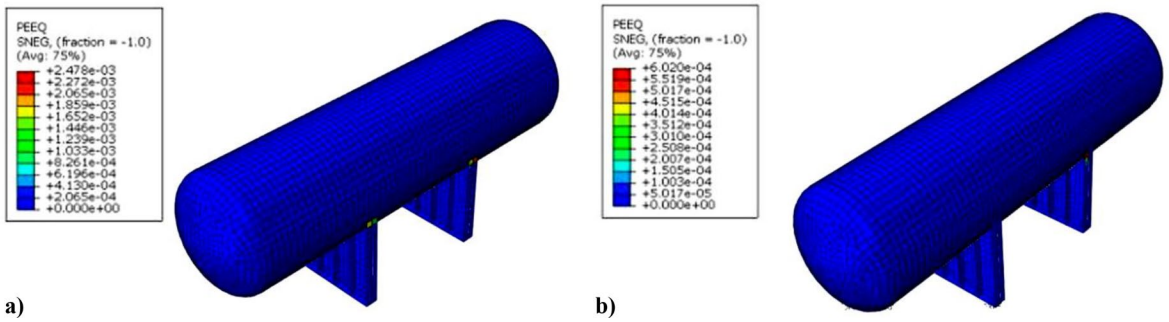

Fig. 16 PEEQ contours for HE1 under GM04 (**a**) uncoupled layout-B and (**b**) coupled

value obtained from the coupled analysis is approximately only 25% of that predicted by the uncoupled analysis. Comparable trends were observed for other ground motions and equipment.

The plastic strain values obtained from the coupled analysis were significantly lower than those from the uncoupled analysis, which can be attributed to the following factors:

- In the uncoupled analyses, the weight of the objects on the platform is estimated and uniformly distributed across the deck area. In contrast, in the coupled model, the equipment is arranged more centrally, resulting in reduced eccentricity compared to the uncoupled model.
- In the uncoupled analysis, the influence of the equipment's mass inertia on its motion is limited due to the imposed fixed boundary conditions. However, in the coupled model, the inertia of the equipment contributes to the overall dynamic response, providing a stabilizing effect during seismic events.

7 Conclusion

This study examines the effects of offshore earthquakes on vessels situated on offshore structures. A representative offshore platform, commonly used in the energy industry, along with five operational hydrocarbon vessels, was modeled using finite element analysis (FEA) software and subjected to uncoupled dynamic simulations.

The dynamic analyses employed 22 ground motion records encompassing a broad spectrum of seismic parameters, including magnitude, peak ground acceleration (PGA), peak ground velocity (PGV), fault distance, and frequency content. The results primarily focus on the maximum plastic strain experienced by the vessels. The key findings can be summarized as follows:

- The results indicate that higher peak ground acceleration (PGA) values and longer ground motion durations tend to be associated with increased PEEQ in the vessel supports located on the upper deck. The relationship between PGA and PEEQ had an R^2 value of 0.44, while the relationship between ground motion duration and PEEQ had an R^2 value of 0.52. These R^2 values suggest moderate correlations, indicating that other factors—such as equipment geometry, soil-structure interaction, plate thickness, material properties, and the frequency content of the ground motion—may also play a significant role in determining the plastic deformation experienced by the vessel supports.
- While PGV and PGA/PGV ratios significantly affect the structural performance of the fixed platform, they do not show a strong correlation with the damage sustained by the vessels on the upper deck.
- Horizontally oriented vessels supported by two saddles are more susceptible to lateral impacts than to longitudinal ones, regardless of the first-mode shape of free vibration.
- The results indicate that displacement pulses caused by forward-directivity effects contribute to plastic strain formation in vessel supports, independent of vessel geometry or support type.
- The coupled model does not always experience displacement pulses, suggesting that objects with shorter natural periods tend to respond dynamically as part of the main structure, rather than exhibiting independent seismic performance, and thus may fail together with the primary system.
- The observed differences between coupled and uncoupled system responses underscore the necessity of evaluating the seismic performance of fixed offshore structures and their onboard equipment using coupled modeling, in addition to traditional uncoupled analyses.
- The comparison of plastic strain results across the five equipment types revealed a trend where larger equipment dimensions generally correlated with higher plastic strain values under seismic loading.
- To gain a more comprehensive understanding of size and plate thickness effects, future research could incorporate a wider range of equipment geometries and

material properties. This would provide a more robust dataset for developing predictive models and design methodologies.

Design recommendations:

- Minimum peak ground acceleration (PGA) values that induce damage in vessel supports are recommended as follows: for seismic design, 0.6 g longitudinally and 0.5 g transversely for HE1; 0.5 g in both directions for HE2; 0.3 g for the VE1; and 0.5 g for the VE3. The current dimension of vessel supports are vulnerable to withstand seismic effects exceeding these parameters. Conventional design approaches may not be adequate, and specialized seismic design regulations should be applied to equipment exposed to ground motions beyond these thresholds.
- It was observed that the outer stiffeners of horizontal saddles experience approximately 2 to 5 times more plasticity than the inner stiffeners. Therefore, the saddle design used in this study is not effective against seismic effects. In addition to the overall inadequacy of the saddle cross-sections, the design should be revised to incorporate outer stiffeners that are 2 to 5 times larger.

Author Contributions A.H. performed the numerical simulations, data analysis, and wrote the original draft. S.O. conceptualized the study, and contributed to the methodology development. B.E. provided technical guidance, supervised the research, and contributed to the discussion section. A.S. reviewed the methodology, provided critical feedback, and helped shape the research. All authors contributed to the manuscript revision and approved the submitted version.

Data Availability No datasets were generated or analysed during the current study.

Declarations

Competing Interests The authors declare no competing interests.

References

Alothman A, Mangalathu S, Hashemi J, Al-Mosawe A, Alam MDM, Allawi A (2021) The effect of ground motion characteristics on the fragility analysis of reinforced concrete frame buildings in Australia. Structures 34:3583–3595. https://doi.org/10.1016/j.istruc.2021.09.084

Amaechi CV, Reda A, Butler HO, Ja'e IA, An C (2022) Review on fixed and floating offshore structures. Part I: types of platforms with some applications. J Mar Sci Eng 10:1074. https://doi.org/10.3390/jmse10081074

American Petroleum Institute (2014) Seismic Design Procedures and Criteria for Offshore Structures, API RP 2EQ (2014)

American Petroleum Institute (2016) Recommended Practice for Design of Offshore Facilities Against Fire and Blast Loading, API RP 2FB (2016)

Ayele YZ, Barabadi A Risk Based Inspection of Offshore Topsides Static Mechanical Equipment in Arctic Conditions, 2016 IEEE International Conference on Industrial Engineering and, Management E (2016) (IEEM), Bali, Indonesia, 2016, pp. 501–506. https://doi.org/10.1109/IEEM.2016.7797926

Bhardwaj S, Ratnayake RMC, Keprate A, Ficquet X (2020) Machine learning approach for estimating residual stresses in girth welds of topside piping, Proceedings of the ASME 2020, 39th International Conference on Ocean, Offshore and Arctic Engineering OMAE2020, June 28-July 3, 2020, Fort Lauderdale, FL, USA

Bommer JJ, Scott SG (2000) The feasibility of using real accelerograms. for Seismic Design Implications of Recent Earthquakes on Seismic Risk

Chakrabarti SK (2005) Handbook of offshore engineering, elsevier, the boulevard, Langford lane, kidlington, Oxford OX5 IGB, UK Radarweg 29. PO Box 2 1 1, 1000 AE Amsterdam, The Netherlands.

Das DK (2019) Understanding MAWP and high-pressure vessel design, ioMosaic, ISO 9001. https://iomosaic.com/docs/default-source/papers/understanding-mawp-and-high-pressure-vessel-design.pdf?sfvrsn=6c2c6d4_8/, (Accessed 09.06.2025)

Dassault Systemes. Abaqus. Retrieve from (2017) http://www.3ds.com/products-services/simulia/products/abaqus/

El-Din MN, Kim J (2015) Seismic performance evaluation and retrofit of fixed jacket offshore platform structures. J Perform Constr Facil 29. https://doi.org/10.1061/(ASCE)CF.1943-5509.0000576

Gazi H, Alhan C (2019) Reliability of elastomeric-isolated buildings under historical earthquakes with/without forward-directivity effects. Eng Struct 195:490–507. https://doi.org/10.1016/j.engstruct.2019.05.081

Gerwick BC (2007) Construction of marine and offshore structures. CRC Press, Taylor & Francis Group. 6000 Broken Sound Parkway NW

Hamidi H, Karbassi A, Lestuzzi P (2020) Seismic response of RC buildings subjected to fling-step in the near-fault region. Struct Concrete 21(5):1919–1937. https://doi.org/10.1002/suco.201900028

Hernandez DH, Larkin T, Chouw N (2017) Influence of base plate bending stiffness on the seismic performance of liquid storage tanks. Procedia Eng 199:170–175. https://doi.org/10.1016/j.proeng.2017.09.214

Huseynli A (2022) Evaluation of Seismic Response of Topside Equipment at Fixed Offshore Platforms, M.Sc. Thesis, Istanbul Technical University, Graduate School, Department of Civil Engineering

ISO 19901-2 2004, Petroleum and natural gas industries-Specific requirements for offshore structures, 1st Edition, ISO/TC 67/SC 7

Kalkan E, Kunnath K (2006) Effects of fling step and forward directivity on seismic response of buildings. Earthq Spectra 22(2):367–390. https://doi.org/10.1193/1.2192560

Katsanos EI, Sextos AG, Manolis GD (2010) Selection of earthquake ground motion records: A state-of-the-art review from a structural engineering perspective. Soil Dyn Earthq Eng 30:157–169. https://doi.org/10.1016/j.soildyn.2009.10.005

Kee TK, Cheok CJ, Kamarudin MAA, Ahmad SW, Suryanti R (2023) Seismic effect of the offshore structure under different earthquake loadings. Int J Integr Eng 15(2):256–262. https://doi.org/10.30880/ijie.2023.15.02.025

Kim SK, Roh MI, Kim KS (2017a) Evaluation of feasibility index in the arrangement design of an offshore topside based on the automatic transformation of experts' knowledge and the fuzzy logic. Ocean Eng 130:284–299. https://doi.org/10.1016/j.oceaneng.2016.11.057

Kim SK, Roh MI, Kim KS (2017b) Arrangement method of offshore topside based on an expert system and optimization technique. J Offshore Mech Arctict Eng 139. https://doi.org/10.1115/1.4035141

Korndörfer J, Hoffmeister B, Feldmann M (2017) Seismic fragility of horizontal pressure vessels - effects of structural interaction between industrial components, COMPDYN 2017, 6th ECCOMAS Thematic Conference on Computational Methods in Structural Dynamics and Earthquake Engineering M. Papadrakakis, M. Fragiadakis (eds.) Rhodes Island, Greece, 15–17 June 2017

Murugan N, Kaliveeran V, Raveesh RM, Kundapura S (2023) Experimental and numerical studies on the stiffening of tubular tjoint of offshore jacket structures. Iran J Sci Technol Trans Civil Eng 48:1373–1393. https://doi.org/10.1007/s40996-023-01236-1

Öztürk S, Sari A (2024) Seismic vulnerability assessment of spherical and horizontal-cylindrical storage tanks through finite element analyses and observational data. Int J Press Vessels Pip 209. https://doi.org/10.1016/j.ijpvp.2024.105214

Öztürk S, Doran B, Aksoylar C (2023) Effect of time step interval and time integration schemes in Pseudo-Dynamic analysis. Structures 50:215–230. https://doi.org/10.1016/j.istruc.2023.02.013

Pachaiappan S, Chandrasekaran S (2022) Numerical analysis of offshore topside with FGM under impact loads. Innovative Infrastructure Solutions 7:195. https://doi.org/10.1007/s41062-022-00802-2

Pappa P, Varelis GE, Vathi M, Perdikaris PC, Karamanos SA (2013) Structural safety of industrial steel tanks, pressure vessels and piping systems under seismic loading (INDUSE)

Peer (2022) Peer ground motion database. Pacific Earthquake Engineering Research Center. https://ngawest2.berkeley.edu/ (accessed January 2022)

Randolph M, Gourvenec S (2011) Offshore Geotechnical Engineering, Spon Press an imrint of Taylor & Francis, 2 Park Square, Milton Park, Abingdon, Oxon OX14 4RN

Rathje EM, Faraj F, Russell S, Bray JD (2004) Empirical relationships for frequency content parameters of earthquake ground motions. Earthq Spectra 20(1):119–144. https://doi.org/10.1193/1.1643356

Ratnayake RMC (2018) Integrity assessment and control of offshore topside piping: an expert system based approach, Proceedings of the ASME 2018, 37th International Conference on Ocean, Offshore and Arctic Engineering OMAE2018, June 17–22, 2018, Madrid, Spain

Sari A, Sayin B, Khiavi MP (2021) A methodology to prevent process piping failures during vapor cloud explosions. Int J Press Vessels Pip 193. https://doi.org/10.1016/j.ijpvp.2021.104436

Sawada T, Hirao K, Yamamoto H, Tsujihara O (1992) Relation Between Maximum Amplitude Ratio and Spectral Parameters of Earthquake Ground Motion, 10th World Conference of Earthquake Engineering. Madrid, Spain, vol. 2

Sehhati R, Rodriguez-Marek A, ElGawady M, Cofer WF (2011) Effects of near-fault ground motions and equivalent pulses on multi-story structures. Eng Struct 33(3):767–779. https://doi.org/10.1016/j.engstruct.2010.11.032

Singh SSP, Agarwal JR, Mani N, Taylor (2020) & Francis Group, 6000 Broken Sound Parkway NW, Suite 300 Boca Raton, FL 33487–2742.

Tangtakabi A, Ramesht MH, Pahlaviani AG, Pourrostam T (2023) Investigation on Chloride–Induced corrosion reduction strategies for offshore reinforced concrete structures. Iran J Sci Technol Trans Civil Eng 48:1245–1260. https://doi.org/10.1007/s40996-023-01230-7

Visser RC (1997) Seismic Considerations in Design and Assessment of Platform Topside Facilities, Society of Petroleum Engineers, SPE 38278, 25–27 June 1997, Long Beach, California

Yang ZR, Shou BN, Sun L, Wang JJ (2011) Earthquake response analysis of spherical tanks with seismic isolation. Procedia Eng 14:1879–1886. https://doi.org/10.1016/j.proeng.2011.07.236

Zafarjoo A, Amirabadi R (2023) Evaluation of seismic behavior of damaged offshore jacket platform under the environmental conditions. Int J Maritime Technol 18:25–39